Endocrinology Articles

Endocrinology and Metabolism

6-2-2021

GCM2 Silencing in Parathyroid Adenoma is associated with Promoter Hypermethylation and Gain of Methylation on Histone 3

Priyanka Singh

Sanjay Kumar Bhadada

Divya Dahiya

Uma Nahar Saikia

Ashutosh Kumar Arya

See next page for additional authors

Follow this and additional works at: https://scholarlycommons.henryford.com/endocrinology_articles

Authors

Priyanka Singh, Sanjay Kumar Bhadada, Divya Dahiya, Uma Nahar Saikia, Ashutosh Kumar Arya, Naresh Sachdeva, Jyotdeep Kaur, Arunanshu Behera, Maria Lusia Brandi, and Sudhaker D. Rao

Clinical Research Article

GCM2 Silencing in Parathyroid Adenoma Is Associated With Promoter Hypermethylation and Gain of Methylation on Histone 3

Priyanka Singh,[1] Sanjay Kumar Bhadada,[1] Divya Dahiya,[2] Uma Nahar Saikia,[3] Ashutosh Kumar Arya,[1] Naresh Sachdeva,[1] Jyotdeep Kaur,[4] Arunanshu Behera,[2] Maria Luisa Brandi,[5] and Sudhaker Dhanwada Rao[6]

[1]Department of Endocrinology, Post Graduate Institute of Medical Education and Research (PGIMER), Chandigarh, 160012, India; [2]Department of General Surgery, PGIMER, Chandigarh, 160012, India; [3]Department of Histopathology, PGIMER, Chandigarh, 160012, India; [4]Department of Biochemistry, PGIMER, Chandigarh, 160012, India; [5]Department of Experimental and Clinical Biomedical Sciences, University of Florence, Florence 50121, Italy; and [6]Bone and Mineral Research Laboratory, Henry Ford Hospital, Detroit, Michigan 48202, USA

ORCiD number: 0000-0002-0410-8778 (S. K. Bhadada).

Abstract

Context: Glial cells missing 2 (*GCM2*), a zinc finger-transcription factor, is essentially required for the development of the parathyroid glands.

Objective: We sought to identify whether the epigenetic alterations in *GCM2* transcription are involved in the pathogenesis of sporadic parathyroid adenoma. In addition, we examined the association between promoter methylation and histone modifications with disease indices.

Methods: Messenger RNA (mRNA) and protein expression of GCM2 were analyzed by reverse transcriptase–quantitative polymerase chain reaction (RT-qPCR) and immunohistochemistry in 33 adenomatous and 10 control parathyroid tissues. DNA methylation and histone methylation/acetylation of the *GCM2* promoter were measured by bisulfite sequencing and chromatin immunoprecipitation–qPCR. Additionally, we

investigated the role of epigenetic modifications on *GCM2* and DNA methyltransferase 1 (*DNMT1*) expression in parathyroid (PTH)-C1 cells by treating with 5-aza-2′-deoxycytidine (DAC) and BRD4770 and assessed for *GCM2* mRNA and DNMT1 protein levels.

Results: mRNA and protein expression of GCM2 were lower in sporadic adenomatous than in control parathyroid tissues. This reduction correlated with hypermethylation (*P* < .001) and higher H3K9me3 levels in the *GCM2* promoter (*P* < .04) in adenomas. In PTH-C1 cells, DAC treatment resulted in increased *GCM2* transcription and decreased DNMT1 protein expression, while cells treated with the BRD4770 showed reduced H3K9me3 levels but a nonsignificant change in *GCM2* transcription.

Conclusion: These findings suggest the concurrent association of promoter hypermethylation and higher H3K9me3 with the repression of *GCM2* expression in parathyroid adenomas. Treatment with DAC restored *GCM2* expression in PTH-C1 cells. Our results showed a possible epigenetic landscape in the tumorigenesis of parathyroid adenoma and also that DAC may be a promising avenue of research for parathyroid adenoma therapeutics.

Key Words: primary hyperparathyroidism, glial cells missing 2, promoter hypermethylation, histone methylation, chromatin immunoprecipitation, 5-aza-2′-deoxycytidine

Primary hyperparathyroidism (PHPT) occurs because of the enlargement of one or more parathyroid glands, which causes overproduction of parathyroid hormone (PTH) (1). However, there is limited literature on the molecular mechanism involved in parathyroid tumorigenesis. Glial cells missing 2 (*GCM2*) is a master regulator required for the development of parathyroid glands in mammals (2-4). In *GCM2*-knockout mice, missing parathyroid glands develop hypocalcemia and hyperphosphatemia, as observed in hypoparathyroidism (5). Since parathyroid glands are not formed in *GCM2*-knockout mice, parathyroid precursor cells undergo apoptosis and die soon after birth (3, 6).

GCM2 is a zinc-type nuclear transcription factor containing a DNA binding domain at the N-terminus that binds to the consensus motif 5′-ATGCGGGT-3′ (2, 7-9). *GCM2* is known to be expressed in parathyroid glands; however ,the downstream targets of *GCM2* and its deregulation in parathyroid adenomas have not been explored (10). Inactivating mutations in the *GCM2* gene can lead to decreased secretion of PTH, resulting in congenital isolated hypoparathyroidism (5, 11, 12).

In silico studies have shown that transcription factors, that is, GCM2-functional binding elements, are present in the calcium-sensing receptor (*CASR*) promoter 1 (−451 to −441 bp relative to the transcription start site [TSS]) and promoter 2 (−166 to −156 bp relative to the TSS), and are able to transactivate *CASR* expression (13-15). Previous studies reported decreased *GCM2* expression both in vivo in mice and in human parathyroid cultured cells treated with *GCM2* small interfering RNA that is associated with

reduction of the *CaSR* gene, a marker of differentiation for parathyroid cells (16).

It has also been demonstrated that *GCM2* interacts with other transcription factors such as GATA binding protein 3 (*GATA3*) and musculoaponeurotic fibrosarcoma oncogene homolog B (*MAFB*), and determines *PTH* expression in cultured cells (8). Nucleotide sequence analysis revealed binding sites for the transcription factors *GATA3* (−55 to −18 relative to the TSS) and paired box 1 (*PAX1*; +8 to +17 relative to the TSS), on the promoter region of *GCM2*, and *GATA3* and *PAX1* both are essential for parathyroid gland development during embryogenesis (17, 18). However, little is known about the molecular mechanisms involved in the transcriptional regulation of *GCM2* and in the downstream activities of GCM2 protein in normal parathyroid tissue or why there is decreased *GCM2* expression in cultured parathyroid cells isolated from chronic kidney disease patients (14). Hence, we asked whether epigenetic modifications such as DNA methylation and histone posttranslational changes regulate *GCM2* expression. DNA methylation is mediated by DNA methyltransferases (DNMTs) that modify cytosine-guanine dinucleotide (CpG) sites, which may result in gene silencing (19). Histone modifications are posttranslational changes to DNA packaging histone proteins that promote chromatin remodeling and changes in gene expression. Methylation and acetylation are the 2 well-characterized histone modifications associated with transcriptional repression and activation of many other target genes. Because of the reversibility of epigenetic modifications, pharmacological agents like 5-aza-2′-deoxycytidine (DAC) and BRD4770 are used to reverse this

process, making them perfect targets for prevention and therapy. The potent and specific DNA methylation inhibitor is DAC, a deoxyribose analogue of nucleoside that is converted to deoxynucleotide triphosphate and is then incorporated in place of cytosine into replicating DNA (20). DAC is used to inhibit DNA methylation in tumor cells and helps to increase the transcription of CASR in colon cancer (21, 22). The formal name of BRD4770 is 2-(benzoylamino)-1-(3-phenylpropyl)-1H-benzimidazole-5-carboxylic acid, and it is used as a histone methyltransferase. Using specific concentrations of BRD4770 will decrease demethylation and trimethylation of lysines on histone 3. A previous study on pancreatic cancer showed the expected effects of BRD770, as it stops the proliferation of pancreatic cancer cells without resulting in apoptosis (23).

Accordingly, in the present study we explored whether DNA methylation and histone modifications affect the regulation of *GCM2* and promote parathyroid tumorigenesis. In addition, we explored the mechanism of epigenetic control of *GCM2* by using DNA and histone methyltransferase–inhibiting drugs in a rat cell line model of parathyroid adenoma, and assessed the effects on *GCM2* mRNA expression.

Materials and Methods

Baseline Participant Characteristics

Participants were enrolled, sampled, and analyzed after giving written informed consent. This study was approved by the institutional ethics committee at the Post Graduate Institute of Medical Education and Research, Chandigarh, India. Participants were diagnosed with PHPT if they presented with elevated plasma PTH and hypercalcemia. A family history suggestive of genetic forms of PHPT such as multiple endocrine neoplasia 1 (MEN1), multiple endocrine neoplasia type 2A (MEN2A), multiple endocrine neoplasia type 4 (MEN4), familial hypocalciuric hypercalcemia syndrome, neonatal severe hyperparathyroidism, HPT-jaw tumor, and familial isolated PHPT were excluded from the study. The differential diagnosis can also be assisted by clinical features, and those related to genetic PHPT were excluded by appropriate clinical examination such as acromegaly, galactorrhea, neurofibromatosis, thyroid cancer surgery, jaw tumor, and appropriate hormonal measurements (serum prolactin and insulin-like growth factor 1). However, gene testing of MEN1 is the desired diagnostic criterion because it identifies germline mutations even without apparent family history of PHPT.

In total, we collected 40 tissue samples from PHPT patients with histologically confirmed parathyroid adenoma (PA) and, from 10 patients, normal parathyroid (control)

during required thyroid surgeries. The tissue samples were routinely fixed in 10% buffered formalin and processed for hematoxylin and eosin stain in the department of histopathology of the institution. The slides were examined to confirm the diagnosis either as adenoma or as normal parathyroid tissue by an experienced endocrine pathologist (U.N.S.).

For each sample, relevant clinical details were recorded and biochemical measurements such as serum calcium (reference range [RR], 8.2-10.2 mg/dL), serum phosphorus (RR, 2.7-4.5 mg/dL), serum creatinine (RR, 0.50-1.20 mg/dL), serum albumin (RR, 3.5-5.5 g/dL), and alkaline phosphatase (RR, 40-129 U/L) were measured by an Olympus autoanalyzer, and the serum calcium level was adjusted with the serum albumin level. Plasma intact PTH (iPTH; RR, 15-65pg/mL) and 25-hydroxyvitamin D (RR, 11.1-42.9 ng/mL) were measured using immunochemiluminescence (ELECSYS-2010; Roche Diagnostics).

Multiple endocrine neoplasia 1 (MEN1) Screening of Study Participants and In Silico Analysis of the Pathogenic Effect of MEN1 variants

MEN1 mutation screening was performed for all study participants from the genomic DNA samples. DNA was isolated from the patient's blood using a Qiagen DNA isolation kit and subjected to polymerase chain reaction (PCR) amplification of all coding exons of the *MEN1* gene. The *MEN1* mutations were identified by Sanger sequencing. Post sequencing, the chromatograms were visualized and analyzed using the CodonCode Aligner. Patients with a *MEN1* variation were further studied; each variation was analyzed in silico for any possible benign or pathogenic effect using the MutPred bioinformatics tool (http://mutpred.mutdb.org/). Only patients with no *MEN1* mutation (n = 33) were included in this study to rule out a genetic contribution to disease pathology.

Analysis of Glial Cells Missing 2 and DNA Methyltransferase 1 Gene Expression

Total RNA was isolated from each parathyroid adenoma and normal parathyroid tissue and reverse transcribed as described previously (24). *GCM2* and *DNMT1* mRNA levels were quantified by reverse transcriptase–quantitative PCR (RT-qPCR) on an ABI StepOnePlus Real-Time PCR System (Applied Biosystems) using *18s* ribosomal RNA as a housekeeping gene for normalization and specific primers: *GCM2* forward primer 5′AAGGCATGCCCTAACTGTCA-3′ and *GCM2* reverse primer 5′ATGAACTCCCTTGGCCTGAA-3′; *DNMT1* forward primer 5′TACCTGGACGACCCTGACCTC-3′ and

DNMT1 reverse primer 5′-CGTTGGCATCAAAGATGG ACA-3′. RT-qPCR reaction conditions were similar to those described in our previous article (25). Experiments were performed in duplicate with 2 nontemplate controls as a negative control. The $2^{-\Delta\Delta CT}$ method was used to quantify the relative expression of *GCM2* and *DNMT1* as a fold change.

Immunohistochemistry

The paraffin-embedded parathyroid adenoma and normal parathyroid tissue blocks were retrieved from the Department of Histopathology and 4- to 5-μ sections were cut for immunohistochemistry (IHC). The IHC protocol was performed as described previously (26). Slides were graded semiquantitatively based on the percentage of positive cells and staining intensity by an endocrine pathologist (U.N.S.) for GCM2 (Abcam, catalog No. ab201170, RRID:AB_2891136 [27]) protein expression. Nuclear staining for GCM2 was regarded as positive. Approximately 200 cells were counted in 6 different regions for each section under 40× magnification. The staining intensity for the parathyroid adenoma and normal parathyroid samples was assessed and graded semiquantitatively: weakly positive (+; < 40%), moderately positive (++; 40%-60%), and strongly positive (+++; > 60%) (24).

Bisulfite-Specific Polymerase Chain Reaction and Sequencing

Genomic DNA from parathyroid adenoma and normal parathyroid tissues were isolated and bisulfite-converted by using the EZ DNA Methylation-Gold Kit (Zymo Research Corp) as previously described (25).

For bisulfite-specific PCR, bisulfite-converted DNA was amplified by using specific primer sets for *GCM2*: forward primer 5′-TTTGGGTAATAGAGTGAGATAA AAA-3′ and reverse primer 5′-AAAAACTAAAAACAAT AATTATAAACCC-3′. Primers were used to amplify the 365-bp sequence containing 17 CpG sites located at nucleotides (nts) −300 to +240 relative to the *GCM2* TSS. PCR reaction was carried out using EpiTaq polymerase enzyme (Takara). Amplified PCR products were separated by electrophoresis on 2% agarose gels and analyzed by bisulfite sequencing (ABI 3730 XL DNA Analyzer; Thermo Fisher Scientific). The sequencing data were evaluated with the online software Bisulfite sequencing and DNA Methylation analysis (BISMA) (25). A methylation density of greater than 10% was considered methylated for the specific gene examined (28).

Chromatin Immunoprecipitation of H3K9me3, H3K27me3, and H3K9ac

Levels of H3K9m3 (Abcam, catalog No. ab8898, RRID:AB_306848 [29]), H3K27me3 (Abcam, catalog No. ab6002, RRID:AB_305237 [30]), and H3K9ac (Cell Signaling Technology, catalog No. 9649, RRID:AB_823528 [31]) on the *GCM2* promoter region were quantified by chromatin immunoprecipitation (ChIP)-qPCR assay. Twenty-three parathyroid adenoma samples were processed for each ChIP-qPCR assay, and the experiment was performed as described previously (22, 32). In brief, 25 to 30 mg of homogenized frozen tissue was fixed with 1% paraformaldehyde at room temperature for 10 minutes, stopped with 0.125-M glycine, and lysed for 10 minutes on ice. The lysate was digested in 1-mL lysis buffer using a tissue homogenizer (NaCl 150 mM, Tris HCl [pH 7.5] 25 mM, EDTA 5 mM, Triton X 100 1%, sodium dodecyl sulfate 0.1%, sodium deoxycholate 0.5%, phenylmethylsulfonyl fluoride 1 mM, and sodium butyrate 10 mM) 1X PIC followed by resuspension in lysis buffer for sonication 15 cycles (30 seconds on and 30 seconds off) using a Diagenode sonicator. Cross-linked DNA was immunoprecipitated with nonspecific immunoglobulin G (IgG) antibodies (45% of total supernatant [Abcam, catalog No. ab171870, RRID:AB_2687657] [33]) for isotype control and immunoprecipitation with anti-H3K9m3, anti-H3K27me3, and anti-H3K9ac antibodies (45% of total supernatant) was performed overnight at 4 °C. The next day, samples were pulled down with protein A/G beads, washed, reverse cross-linked, and ChIP-DNA was extracted with phenol-chloroform isoamyl alcohol as described previously. For ChIP-qPCR assay, primers were designed by using primer blast provided by National Center for Biotechnology Information and sequences used were *GCM2* forward primer 5′-TGTGCTCCTACGGGATGCAG-3′ and *GCM2* reverse primer 5′-CCCTCCTTCGGATGGACAGC-3′. qPCR with ChIP primers was carried out and performed in duplicate, and levels of H3K9me3, H3K27me3, and H3K9ac were calculated by the fold enrichment method relative to the nonspecific antibody and normalized to the input DNA.

Parathyroid-C1 cell line

Because a human parathyroid cell line is not available, the parathyroid-C1 (PTH-C1) cell line, which was established from rat parathyroid tissue, was used for in vitro treatment assays (34). The PTH-C1 cells have an epithelial morphology and exhibit parathyroid functional features (34). The cells were cultured in 25 cm^2 or 75 cm^2 tissue culture flasks supplemented with nutrient mixture F-12 Ham Coon's modification (Sigma-Aldrich) containing 10% fetal bovine

serum (Gibco, Thermo Fisher Scientific), and 100-U/mL penicillin/streptomycin (Gibco, Thermo Fisher Scientific) and then incubated at 37 °C in a 5% CO_2 incubator.

In vitro treatments and 3-(4, 5-dimethylthiazol-2-yl)-2,5-diphenyl tetrazolium bromide assay

A stock solution of DAC or BRD4770 (Sigma-Aldrich) was made in vehicle and diluted to appropriate concentrations for treatment. Cells treated with vehicle control were taken as controls. Approximately 1×10^4 cells were seeded per well in a 96-well plate and then subsequently treated with different concentrations of DAC for 72 hours and BRD4700 for 48 hours alone, respectively. At the end of the treatments, 100 μL of 3-(4, 5-dimethylthiazol-2-yl)-2,5-diphenyl tetrazolium bromide (MTT) reagent was added to each well from a 5-mg/mL stock in phosphate-buffered saline (PBS). The 96-well plates were incubated for 3 hours at 37 °C in the dark. The supernatant was taken out and formazan crystals were dissolved in 100-μL dimethyl sulfoxide at 37 °C for 10 minutes with gentle agitation. Absorbance from the plates was read at 570 nm and reference was read at 620 nm with an enzyme-linked immunosorbent assay reader.

Impact of 5-aza-2′-deoxycytidine treatment on glial cells missing 2 expression in parathyroid-C1

To study the impact of DAC on the expression of *GCM2* in PTH-C1 cells by RT-qPCR, cells were treated with 10-μM DAC for 72 hours (the fresh drug was changed every 24 hours). Total RNA was isolated from treated and untreated PTH-C1 cells, reverse transcribed, and *GCM2* mRNA expression was assessed by RT-qPCR as described earlier for tissue samples (25). In treatment experiments, rat-specific *GCM2* primers were used: forward primer 5′-TGCCTCAGGAACCAGCTCACT-3′ and reverse primer 5′-AGGTGGCGCTGAGCTTTCTTC-3′. Experiments were performed in triplicate with 2 nontemplate samples as a negative control. Data were normalized using β-actin (forward primer 5'CCCATCTATGAGGGTTACGC-3′ and reverse primer 5′-TTTAATGTCACGCACGATTTC -3′) as a housekeeping gene and relative expression by fold change was calculated using $2^{-\Delta\Delta CT}$ value.

Impact of BRD4770 treatment on glial cells missing 2 expression in parathyroid-C1

After treatment with 5-μM BRD4770 in PTH-C1 cells for 48 hours, H3K9me3 levels assessed by ChIP-qPCR and mRNA expression of *GCM2* were quantified by RT-qPCR. ChIP-qPCR assay was performed on ChIP-DNA isolated from treated and untreated PTH-C1 cells. Rat-specific *GCM2* primers (forward primer 5′-GGAGCCTGAGGTAATGGGCT-3′ and reverse primer

5′-ATTAGAGCCCCGAGCCAAGG-3′) were used in the qPCR. Finally, ChIP-qPCR was performed, and analysis was carried out as described earlier for human parathyroid tissue samples.

Immunofluorescence staining of DNA methyltransferase 1 in parathyroid-C1 cells

After treatment with DAC, PTH-C1 cells were grown on 8-well glass-chambered slides and fixed with 4% paraformaldehyde in 1X PBS for 20 minutes, then washed extensively with 1X PBS. Cells were permeabilized with 0.2% Triton-X in 1X PBS for 20 minutes and blocked with 2% bovine serum albumin in PBS for 1 hour. Primary antibodies for proteins of interest (DNMT1; Abcam, catalog No. ab188453, RRID:AB_2877711 [35]) were diluted in 2% bovine serum albumin and applied to the cells. Slides were incubated for 4 hours at room temperature. After washing with 1X PBS, a secondary antibody-labeled fluorochrome (1:500) was applied to the cells for 1 hour at room temperature in the dark. The cells were washed once for 5 minutes with 1X PBS. Nuclear staining and mounting were performed with Anti Fade Gold reagent (Thermo Fisher Scientific). Whole-slide images were acquired using an EVOS microscope with appropriate fluorescent labels.

Statistical analysis

Graph Pad Prism version 6.0 was used to analyze the data. qPCR data are expressed as mean ± SD and ChIP-qPCR data expressed as mean ± SEM. In vitro data represent 3 independent trials and are shown as mean with SEM. A *P* value of less than .05 was considered statistically significant. Mann-Whitney, chi-square, and *t* tests were used as appropriate to compare the differences in study data between the control and adenoma samples. The Pearson correlation test was used to examine the relationship among various continuous variables.

Results

Characteristics of Primary Hyperparathyroidism Patients

The mean age of the patients with confirmed parathyroid adenoma was 43 ± 13.5 years (range, 18-65 years) with a female to male ratio of 3:1 (31 women and 9 men). The mean age of the patients with normal parathyroid function who had undergone required surgery for benign thyroid disease was 43 ± 13.3 years (range, 25-61 years; 7 women and 3 men). The presence of bone pains, weakness, and fatigue, kidney stones, gallstone disease, fractures, pancreatitis, and vitamin D deficiency (25-hydroxyvitamin D level < 20 ng/mL) at the time of presentation was categorized as

symptomatic PHPT. All the patients had hypercalcemia, with mean serum calcium of 12.0 ± 1.0 (RR, 10.5-14.5 mg/dL), elevated median iPTH level of 558 pg/mL (first interquartile range [IQR]-third IQR), and median parathyroid adenoma weight was 2 g (first IQR-third IQR) (22).

Transcriptional Pattern of Glial Cells Missing 2 in Sporadic Parathyroid Adenomas

RT-qPCR analysis showed *GCM2* mRNA levels were significantly lower in 29 (88%) of the 33 sporadic parathyroid adenomas relative to the control parathyroid samples, with a mean fold-change reduction of 0.25 ± 0.25 ($P < .0001$) (Fig. 1A). IHC analysis revealed nuclear staining for GCM2 protein both in the adenomatous and control parathyroid gland samples. In the control parathyroid samples, we observed 3+ intensity. In contrast, in the parathyroid adenomatous samples, we observed 1+ intensity in 16 of 33 (48%), 2+ intensity in 14 of 33 (42%), and 3+ intensity in 3 of 33 (9%) (Fig. 1B). The mean proportion of GCM2-positive cells was 44 ± 22% in sporadic parathyroid adenomas and 77.8 ± 3.4% in the control parathyroid samples. GCM2 protein expression was significantly reduced in the parathyroid adenomas relative to the control parathyroid samples ($P < .0001$).

Glial Cells Missing 2 Promoter Hypermethylation in Sporadic Parathyroid Adenomas

Bisulfite-converted DNA sequence analysis showed that 17 CpG sites (nt −300 to +240 relative to the TSS) located upstream of the *GCM2* promoter (Fig. 2A) had high levels of methylation in 57.5% (n = 19) of the parathyroid adenomas with a mean methylation density of 20.7 ± 6% (range, 11.1%-33.3%). While 14 parathyroid adenomas had a mean methylation density of less than 10%, 3 parathyroid adenomas did not show methylation at any CpG sites in the region of the *GCM2* promoter. Normal control parathyroid samples showed complete methylation at none of the 17 CpG sites, except for a single sample that showed an average of 6.7% methylation. Representative unmethylated and methylated CpG sites in the *GCM2* promoter region are shown in Fig. 2B. The promoter region of *GCM2* in parathyroid adenoma was highly methylated, showing complete methylation at 13 of 17 CpG sites. Also notable in the parathyroid adenomas, the eighth CpG site, which is a putative GATA3 binding site (nt −55 to −18 relative to +1 TSS), showed an average methylation of 56.4%, and the twelfth CpG site, a PAX1 binding site (nt +8 to +17 relative to +1 TSS), showed only 3.4% average methylation (Fig. 2C). Correlation analysis revealed a significant negative association between *GCM2* mRNA expression and the level of methylation in sporadic parathyroid adenomas ($r = −0.52$; $P < .001$) (Fig. 2D). Thus, the reduced expression of *GCM2* in parathyroid adenoma tissues was the effect of the methylation.

DNA Methyltransferase 1 Expression in Parathyroid Adenomas

Because we observed such a high level of methylation in the *GCM2* promoter in parathyroid adenomas, we
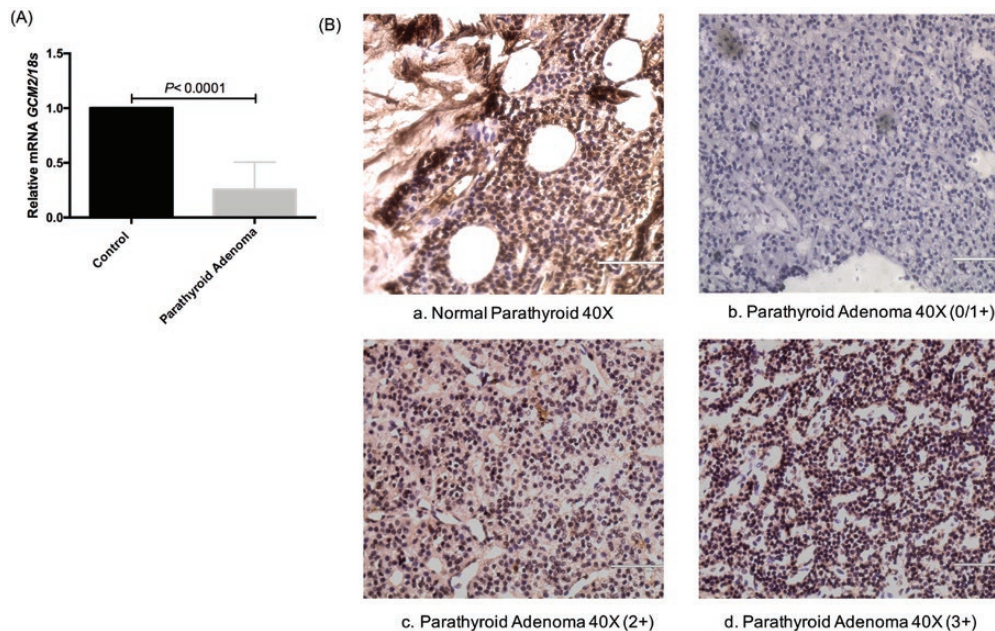

Figure 1. Glial cells missing (*GCM2*) messenger RNA (mRNA) and protein expression analysis in sporadic parathyroid adenoma (N = 33). a, Bar graph representing relative mRNA expression of *GCM2* in parathyroid adenoma compared to control parathyroid samples. b, Representative photomicrographs showing GCM2 protein levels in A, parathyroid tissue sections control, and B, C, and D, show intensity in parathyroid adenoma as 1+, 2+, and 3+, respectively. Images captured at 40× magnification, scale bar = 400 μm.
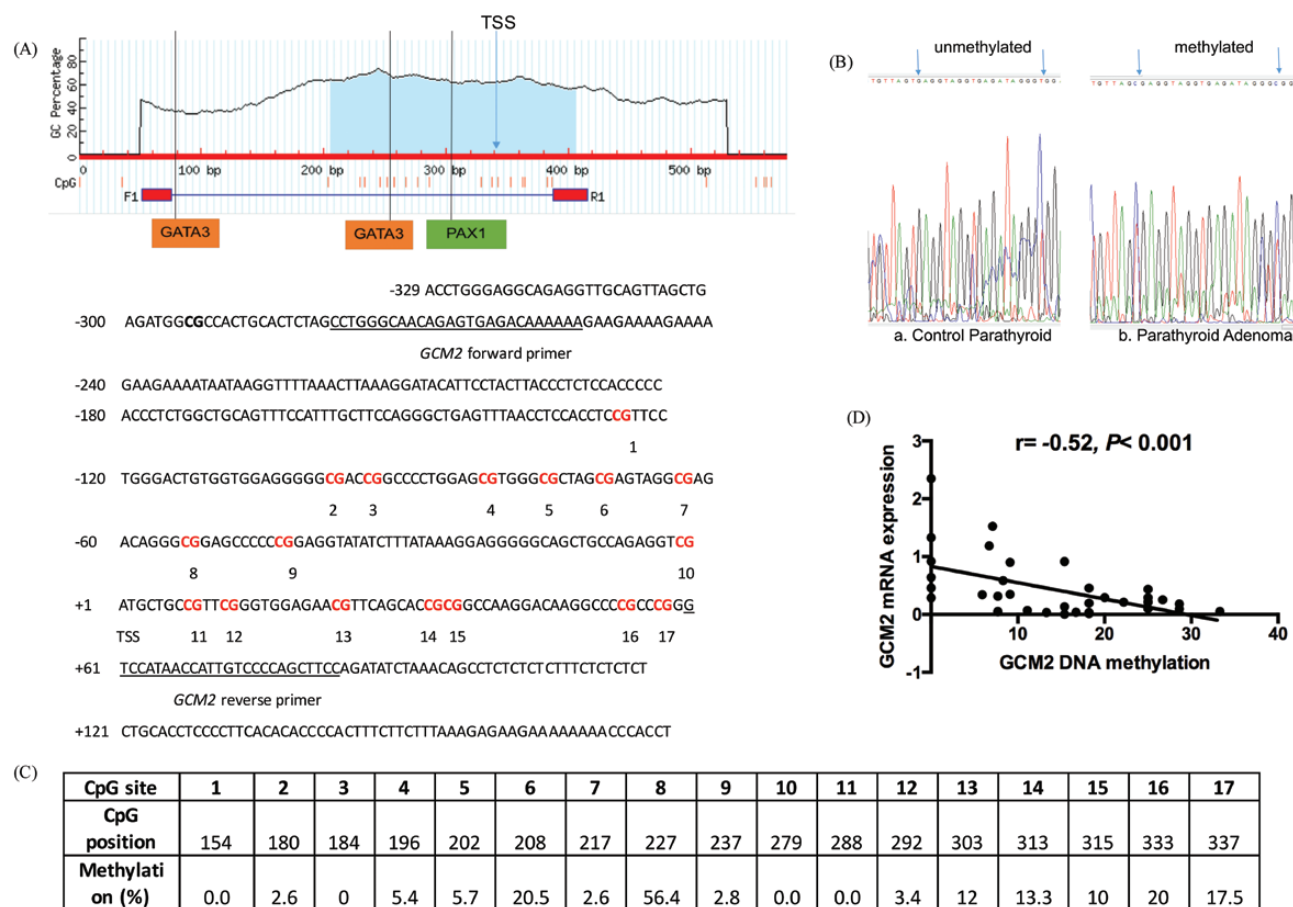
Figure 2. Glial cells missing (*GCM2*) promoter methylation in sporadic parathyroid adenoma (N = 33). A, *GCM2* promoter region selected for bisulfite sequencing polymerase chain reaction showing putative *GATA3* and *PAX1* binding sites and the transcription start site (TSS). B, Representative chromatograms showing methylated sites (blue arrow) in parathyroid adenoma compared to control parathyroid. C, Tabular representation of 17 cytosine-guanine dinucleotide (CpG) sites at *GCM2* promoter showing average percentage methylation at each CpG site. D, Scatter plot showing the negative association between gene expression of *GCM2* and DNA promoter methylation in sporadic parathyroid adenoma cases (N = 33).

next examined the gene expression of the maintenance methyltransferase *DNMT1*. We found that *DNMT1* mRNA levels were significantly upregulated in sporadic parathyroid adenomas, with a mean fold change of 5.1 ± 3.7 ($P < .0006$) compared with the control parathyroid samples (Fig. 3). We found a significantly positive association between *DNMT1* mRNA levels and *GCM2* promoter hypermethylation ($r = 0.39$; $P < .03$) in sporadic parathyroid adenomas. Further, we observed that *DNMT1* mRNA expression was positively associated with tumor weight ($r = 0.40$; $P < .03$), although it was not associated with any other biochemical parameters of parathyroid adenomas.

H3K9me3, H3K27me3, and H3K9ac Modifications in Sporadic Parathyroid Adenomas

Next, we investigated levels of posttranslational methylation and acetylation on histone 3 within the *GCM2* promoter in adenomatous and control parathyroid tissues using 23 adenomas and 10 control parathyroid samples. ChIP-qPCR analysis revealed higher H3K9me3 levels relative to IgG in the *GCM2* promoter in parathyroid adenomas compared to control parathyroid, with a mean fold increase of 7.67 ± 3.08 in parathyroid adenoma and 0.52 ± 0.16 in control parathyroid samples relative to IgG. Levels of H3K27me3 relative to IgG were high in 19 of the 23 (83%) parathyroid adenomas with an overall mean fold increase of 31.2 ± 22.4, whereas the mean increase was only 1.15 ± 0.23 in control parathyroid samples. Thus, sporadic parathyroid adenomas exhibited 15-fold ($P < .02$) and 26-fold ($P < .004$) higher levels of H3K9me3 and H3K27me3, respectively, compared to control parathyroid samples (Fig. 4A and 4B). In contrast, H3K9ac levels were lower in parathyroid adenomas, with mean fold increases of 3.03 ± 0.58 in 20 of the 23 (87%) and 14.6 ± 9.40 in the control parathyroid samples relative to IgG (Fig. 4C). Thus, the active histone marker H3K9ac was decreased by 5-fold ($P < .02$) in sporadic parathyroid adenomas compared to control parathyroid samples.

The Pearson correlation analysis between *GCM2* mRNA expression and H3K9me3 methylation, a repressive modification associated with gene repression, showed a significantly negative association in parathyroid adenomas ($r = -0.49$, $P < .04$). The other repressive modification, H3K27me3, was significantly associated with serum calcium, whereas the activating modification, H3K9ac, showed a significant inverse relationship with plasma iPTH in parathyroid adenomas.

5-Aza 2′-deoxycytidine and BRD4770 cytotoxicity detection using the 3-(4, 5-dimethylthiazol-2-yl)-2,5-diphenyl tetrazolium bromide assay

To detect the cytotoxicity of DAC and BRD4770, we performed the MTT assay. As shown in Fig. 5, there was no significant difference between the experimental group

Figure 3. Bar graph representing relative messenger RNA (mRNA) expression of DNA methyltransferase 1 (*DNMT1*) in parathyroid adenomas compared to control parathyroid samples.

and negative control. We conclude that 10-µM DAC and 5-µM BRD4770 produced no cytotoxicity in PTH-C1 cells, respectively.

Inhibition of DNA Methyltransferase 1 With 5-Aza 2′-Deoxycytidine Results in Higher Glial Cells Missing 2 Transcription in Parathyroid-C1 cells

To test whether inhibition of DNMT1 would result in increased *GCM2* transcription by putatively relieving epigenetic inhibition, we treated the transformed rat parathyroid cell line, PTH-C1, with DAC, and measured the mRNA levels of *GCM2* by RT-qPCR. In PTH-C1 cells, we observed that the expression of *GCM2* was significantly increased ($P < .001$) (Fig. 6A) after treatment with 10-µM DAC for 72 hours relative to untreated cells. Immunofluorescence microscopy revealed reduced protein levels of DNMT1 after treatment with 10-µM DAC for 72 hours in PTH-C1 cells compared to untreated cells (Fig. 6B).

Histone Methylation (H3K9me3) and Glial Cells Missing 2 Expression in Parathyroid-C1 cells in response to BRD4770

Next, to show that treatment with the histone methyltransferase inhibitor BRD4770 affects the H3K9me3 modification within the *GCM2* promoter, a ChIP-qPCR assay was performed to measure H3K9me3 levels. In ChIP-qPCR analysis, we observed a decrease of H3K9me3 levels in the *GCM2* promoter region in BRD4770-treated PTH-C1 cells compared to untreated cells (Fig. 7A). However, we found a slight but not significant increase of *GCM2* mRNA in BRD4770-treated PTH-C1 cells relative to untreated cells (Fig. 7B).
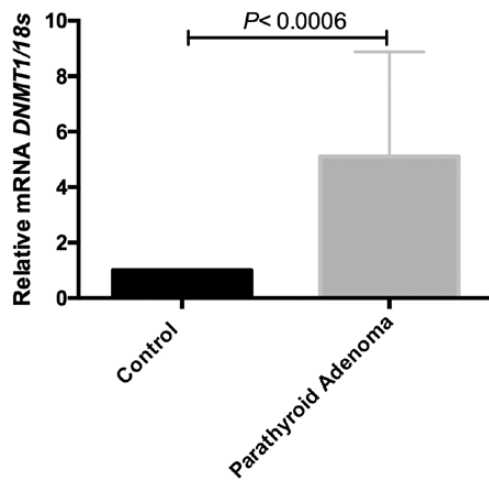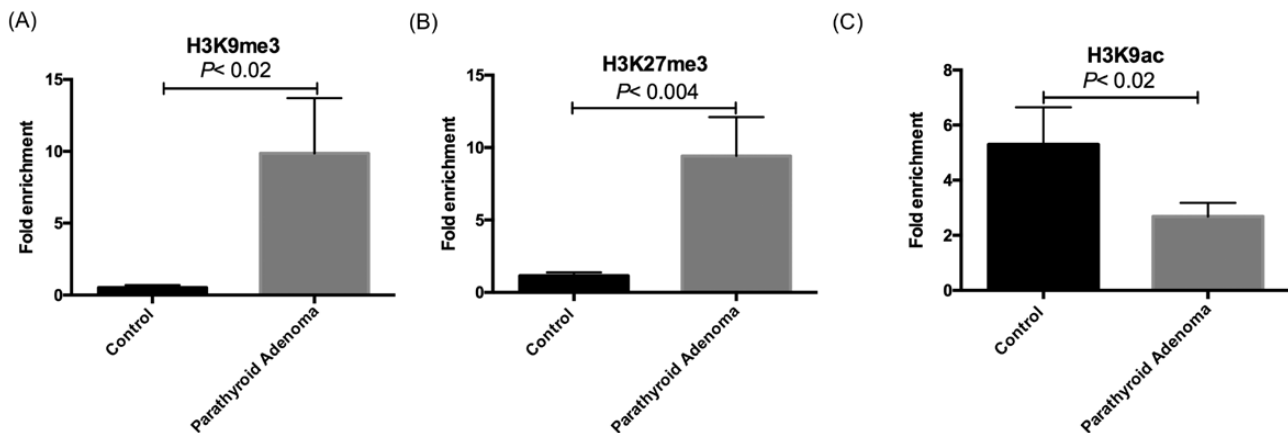
Figure 4. Chromatin immunoprecipitation–quantitative polymerase chain reaction for Glial cells missing (*GCM2*) promoter region in sporadic parathyroid adenomas. Quantification of fold enrichment in A, H3K9me3; B, H3K27me3; and C, H3K9ac (levels relative to nonspecific immunoglobulin G as control and normalized with input DNA). Bars represent mean fold enrichment and SEM (n = 23).
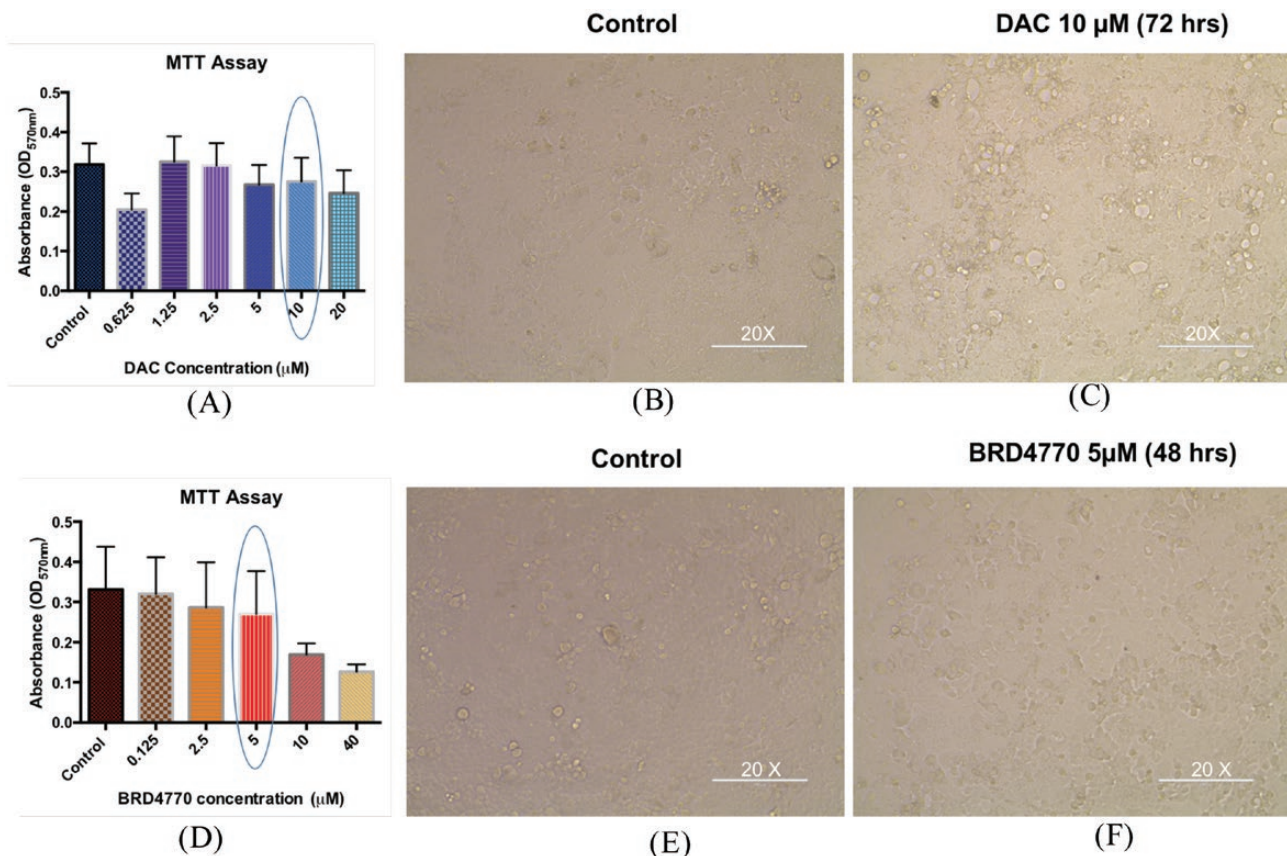
Figure 5. Cell viability was analyzed with 3-(4, 5-dimethylthiazol-2-yl)-2,5-diphenyl tetrazolium bromide (MTT) assay in parathyroid (PTH)-C1 cells after using different concentrations of A, 5-aza 2′ deoxycytidine (DAC) for 72 hours. Data are shown as means of 3 experiments in triplicate ($P < .78$). B and C, Representative bright-field images of control and DAC-treated PTH-C1 cells for 72 hours; and D, 2-(benzoylamino)-1-(3-phenylpropyl)-1H-benzimidazole-5-carboxylic acid (BRD4770), for 48 hours. Data are shown as means of 3 experiments in triplicate ($P < .40$). E and F, Representative bright-field images of control and BRD4770-treated PTH-C1 cells for 48 hours at 20×, scale bar = 200 μM.

Discussion

In the present study, we demonstrate that *GCM2*, a master regulator for parathyroid gland development (36), is hypermethylated in parathyroid adenomas and results in downregulated expression of *GCM2* mRNA. We also found that H3K9me3 and H3K27me3 levels were higher, and H3K9ac was lower, in adenomatous compared to control parathyroid samples. Furthermore, treatment with DAC, a DNA methyltransferase inhibitor, can restore *GCM2* expression in PTH-C1 cells. To our knowledge, this is the first study to fully describe the epigenetic landscape of the *GCM2* promoter in human parathyroid adenomas, and the first to report that promoter DNA hypermethylation contributes to the regulation of *GCM2* in sporadic parathyroid adenomas.

We observed significantly reduced mRNA and protein expression of GCM2 in sporadic parathyroid adenomas relative to control parathyroid samples. These findings are in agreement with previous reports that showed similar underexpression of *GCM2* in parathyroid tumors (14, 37).

One limitation of the present study is that the genetic status of *GCM2* was not analyzed in sporadic parathyroid adenomas. Previous studies by Kebebew and colleagues in 2004 and Mannstadt et al in 2011 showed underexpression or overexpression of the *GCM2* gene in parathyroid adenomas, respectively (10, 38). Activating mutations might account for the overexpression of the *GCM2* gene. Another study by Guan et al in 2016 that studied the genetic status of the *GCM2* identified the non–C-terminal conserved inhibitory domain (CCID) variant in the Italian population; however, it did not appear in Asian/Indian population (39). In a subset of families with familial isolated PHPT, germline-activating mutations affecting the *GCM2* CCID variants were observed (39) and have never been found in MEN1 or HPT-jaw tumor syndrome. Of note, Guan et al in 2017 concluded that *GCM2*-activating variants were seen in the sporadic PHPT patients who had multigland involvement or persistent disease (40). However, Riccardi and colleagues in a 2019 study reported that the known *GCM2*-activating variants may not intend to develop a
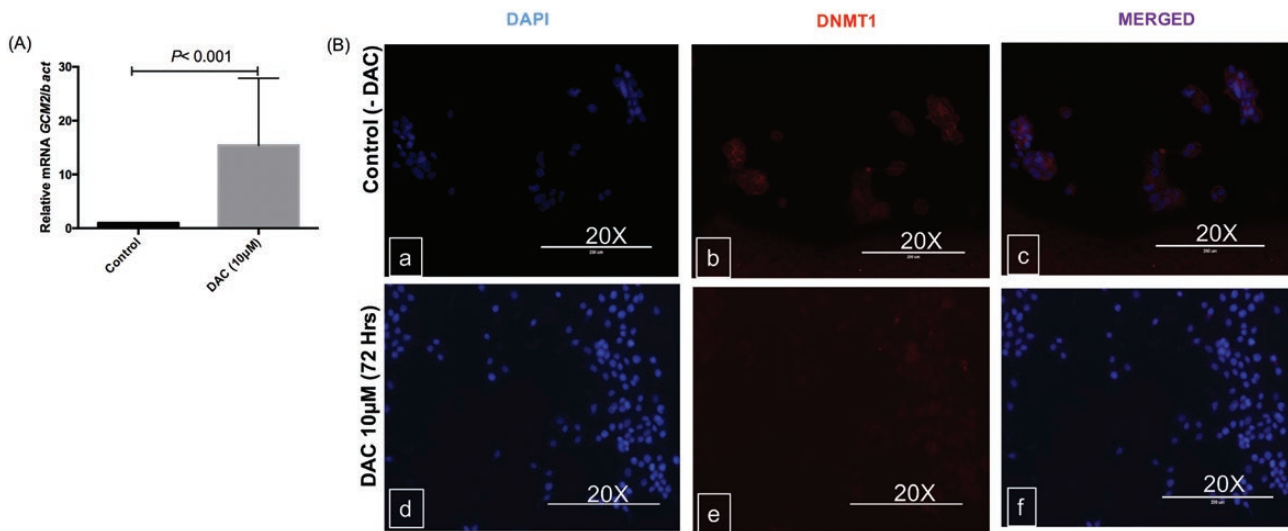
Figure 6. The effect of 5-aza-2′-deoxycytidine (DAC) treatment in a parathyroid cancer cell line (PTH-C1). A, Expression of glial cells missing (*GCM2*) messenger RNA (mRNA) relative to beta actin in PTH-C1 cells treated with 10 μM DAC vs untreated cells at 72 hours as determined by reverse transcriptase–quantitative polymerase chain reaction. The results are shown as mean and SEM values and *P* values were evaluated using *t* test from 3 independent experiments. B, Representative immunofluorescence staining of DNA methyltransferase 1 (DNMT1; red) in PTH-C1 cells (untreated with DAC, upper panel; treated with DAC, bottom panel). Nuclei were stained with 4′, 6-diamidino-2-phenylindole (DAPI; blue). Images captured at 20× magnification. Scale bar = 200 μm.
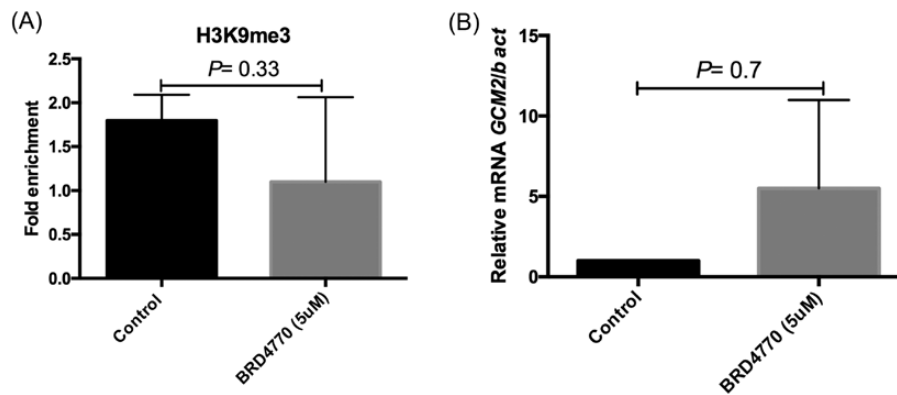

Figure 7. The effect of 2-(benzoylamino)-1-(3-phenylpropyl)-1H-benzimidazole-5-carboxylic acid (BRD4770) treatment in a parathyroid cancer cell line (PTH-C1). PTH-C1 cells were treated with 5 μM of BRD4770 for 48 hours. A, Presence of H3K9me3 modification in the glial cells missing (*GCM2*) promoter quantified by chromatin immunoprecipitation–quantitative polymerase chain reaction. After treatment with BRD4770, decreased in trimethylation of H3K9 level was observed in the GCM2 promoter region. B, Expression of *GCM2* messenger RNA (mRNA) relative to actin in the PTH-C1 cell line before and after BRD4770 treatment. Results are shown as mean and SEM values, and *P* values were evaluated by *t* test from 3 independent experiments.

sporadic adenoma, though increased disease risk would be expected in carriers of such variants compared with the general population (41). But the exact mechanism of deregulated *GCM2* expression in parathyroid tumorigenesis is still undetermined.

Interestingly, Canaff et al in 2007 identified functional *GCM2*-binding sites on *CaSR* promoters (promoter 1 and promoter 2); thus, there appears to be an association between *GCM2* and *CaSR* (14). Our recent study also showed hypermethylation of a CpG site located within the *GCM2*-binding region on the *CaSR* promoter 2 affected

CaSR expression in patients with sporadic parathyroid adenomas (22, 24, 37). Thus, the methylation analysis of a specific CpG site might play a key determinant role in the reduced gene expression. In the present study, the *GCM2* promoter was hypermethylated with a significant inverse relationship between *GCM2* mRNA expression and promoter methylation. Previously, it has been reported that loss of *GCM2* expression in renal cell carcinoma is due to genetic deletions and that tumor-specific methylation correlates with survival (42). The *GCM2* promoter contains putative *GATA3* and *PAX1*-binding sites, and both

are developmental transcription factors that regulate *GCM2* expression (6, 8). A noteworthy observation was that the eighth (*GATA3*-binding site) and twelfth CpG sites (*PAX1*-binding site) showed 57.5% methylation and 3.4% methylation, respectively, in sporadic parathyroid adenoma. Similarly, others have reported that *GATA3* acts via *GCM2* regulation in parathyroid adenomas, as the *GCM2* promoter is enriched with GATA3-binding motifs (6, 43). Another study reported that *GATA3* interacts with *GCM2* and *MAFB* transcription factors resulting in stimulation of *PTH* gene expression (8). Also, there is a strong link between *PAX1* and *GCM2*, as *PAX1* also helps to determine cell fate in the development of the parathyroid glands (17). Our results showed that *GCM2* promoter hypermethylation, as well as specific methylated CpG sites, might lead to steric hindrance for transcription factor (*GATA3* and *PAX1*)-binding, causing decreased *GCM2* expression. This observation is of key interest for future investigations exploring predictive and prognostic biomarkers for sporadic parathyroid adenomas.

Our study showed significantly increased mRNA expression of *DNMT1* in sporadic parathyroid adenomas compared to control parathyroid samples. A previous study on MEN showed DNA hypermethylation to be mediated by enhanced *DNMT1* activity, thereby regulating the transcriptional silencing of menin 1 (*MEN1*). In this study, we found that *DNMT1* expression was strongly associated with *GCM2* promoter methylation patterns in sporadic parathyroid adenomas, suggesting that reduced expression of *GCM2* may be due to DNMT1-mediated methylation. Correlation analysis suggested a significant association between *DNMT1* mRNA expression and tumor weight in sporadic parathyroid adenomas. Earlier reports have suggested giant or large parathyroid tumor size correlates well with the severity of the disease (44, 45). This suggests that large tumor weight results in a more pronounced clinical picture in sporadic PHPT patients, with severe hypercalcemia and elevated iPTH levels.

Additionally, to understand the reason for reduced *GCM2* expression, histone modifications have been studied. However, this is the first study to analyze histone changes in the promoter region of *GCM2* in parathyroid adenoma, and we observed significantly higher H3K9me3 and H3K27me3 levels and lower H3K9ac levels. In a similar manner, we observed a significant inverse relationship of promoter hypermethylation and H3K9me3 levels with reduced *GCM2* expression in sporadic parathyroid adenomas, thus linking both with transcriptional silencing. This is in line with a previous study that reported an interplay of histone modification and DNA methylation in

decreased *RASSF1A* expression in breast cancer (46). Thus, we propose a possible role for H3K9me3 as a chief regulator in parathyroid tumorigenesis that should be investigated further.

We further examined the role of *GCM2* promoter DNA and histone methylation by using the epigenetic inhibition drugs DAC and BRD4770 in the PTH-C1 cell line to observe whether they might cause reactivation of silenced *GCM2* in PTH-C1 cell line. Several reports in colorectal cancer cell lines such as HCT116, SW48, and SW480 have shown that DAC treatment inhibits DNMT1 activity, causing reexpression of genes such as clusterin, interleukin-23 receptor, transketolase-like 1, and tubulin α-3C (47). We saw a reduction of DNMT1 protein in DAC-treated PTH-C1 cells and a concomitant significant increase in *GCM2* gene expression after DAC treatment. The restoration of *GCM2* expression suggests that inhibition of DNMT1 is sufficient and necessary to activate the *GCM2* promoter. Previous studies have reported that DAC has been recognized as a therapeutic epigenetic-modifying drug and has been approved for the treatment of cancer (21, 47, 48).

In addition, we also further explored the role of H3K9me3 in PTH-C1 cells, since increased H3K9me3 levels were observed in the *GCM2* promoter in human sporadic parathyroid adenomas. Thus, PTH-C1 cells treatment with BRD4770 resulted in lower H3K9me3 levels in the *GCM2* promoter as observed by ChIP-qPCR, but changes in *GCM2* transcription were not significantly different between treated and untreated cells, despite a trend suggestive of increased expression. BRD4770 has shown success in reducing H3K9me3 levels in pancreatic and liver cancer cells without inducing apoptosis (23).

The data on PTH-C1 cells, while not significant, may indicate a promising topic for future, more detailed research on the role of H3K9me3 histone modification in parathyroid disease.

Taken together, DNA hypermethylation and higher histone H3K9me3 levels in the *GCM2* promoter in sporadic parathyroid adenomas both suggest that epigenetic modifications play a key role in the transcriptional silencing of *GCM2*, perhaps contributing to parathyroid tumorigenesis.

The limitations of this study, first, we did not determine the genetic status of the *GCM2* gene in sporadic parathyroid adenomas. Second, in vitro experiments were performed in the rat parathyroid cell line PTH-C1 (34). As of yet, there is no human parathyroid cell line available for ideal in vitro experiments; however, transformed rat parathyroid cell lines may serve as an excellent model to study potential therapeutics. Third, protein expression of DNMT1 was not performed in parathyroid adenomas.

Conclusion

Our results demonstrate for the first time the importance of epigenetics in downregulating the expression of *GCM2* through its promoter hypermethylation and histone methylation in human sporadic parathyroid adenomas. Strategies to upregulate *GCM2* expression by targeting DNA and histone methylation may be useful to prevent and/or treat sporadic parathyroid adenoma.

Acknowledgments

Additional Information

Correspondence: Sanjay Kumar Bhadada, MD, DM, Department of Endocrinology, Post Graduate Institute of Medical Education and Research, Chandigarh 160012, India. Email: bhadadask@rediffmail.com.

Disclosures: The authors have no potential conflicts of interest to disclose.

Data Availability: All relevant data are within in the manuscript. The data sets generated during and/or analyzed during the present study are available from the corresponding author on reasonable request.

References

1. Bhadada SK, Arya AK, Mukhopadhyay S, et al. Primary hyperparathyroidism: insights from the Indian PHPT registry. *J Bone Miner Metab.* 2018;**36**(2):238-245.

2. Kanemura Y, Hiraga S, Arita N, et al. Isolation and expression analysis of a novel human homologue of the Drosophila glial cells missing (*gcm*) gene. *FEBS Lett.* 1999;**442**(2-3):151-156.

3. Günther T, Chen ZF, Kim J, et al. Genetic ablation of parathyroid glands reveals another source of parathyroid hormone. *Nature.* 2000;**406**(6792):199-203.

4. Maret A, Ding C, Kornfield SL, Levine MA. Analysis of the *GCM2* gene in isolated hypoparathyroidism: a molecular and biochemical study. *J Clin Endocrinol Metab.* 2008;**93**(4):1426-1432.

5. Thomée C, Schubert SW, Parma J, et al. GCMB mutation in familial isolated hypoparathyroidism with residual secretion of parathyroid hormone. *J Clin Endocrinol Metab.* 2005;**90**(5):2487-2492.

6. Grigorieva IV, Thakker RV. Transcription factors in parathyroid development: lessons from hypoparathyroid disorders. *Ann N Y Acad Sci.* 2011;**1237**:24-38.

7. Chuang HC, Chang CW, Chang GD, Yao TP, Chen H. Histone deacetylase 3 binds to and regulates the GCMa transcription factor. *Nucleic Acids Res.* 2006;**34**(5):1459-1469.

8. Han SI, Tsunekage Y, Kataoka K. Gata3 cooperates with Gcm2 and MafB to activate parathyroid hormone gene expression by interacting with SP1. *Mol Cell Endocrinol.* 2015;**411**:113-120.

9. Cohen SX, Moulin M, Schilling O, et al. The GCM domain is a Zn-coordinating DNA-binding domain. *FEBS Lett.* 2002;**528**(1-3):95-100.

10. Mannstadt M, Holick E, Zhao W, Jüppner H. Mutational analysis of GCMB, a parathyroid-specific transcription factor, in parathyroid adenoma of primary hyperparathyroidism. *J Endocrinol.* 2011;**210**(2):165-171.

11. Ding C, Buckingham B, Levine MA. Familial isolated hypoparathyroidism caused by a mutation in the gene for the transcription factor GCMB. *J Clin Invest.* 2001;**108**(8):1215-1220.

12. Mannstadt M, Bertrand G, Muresan M, et al. Dominant-negative GCMB mutations cause an autosomal dominant form of hypoparathyroidism. *J Clin Endocrinol Metab.* 2008;**93**(9):3568-3576.

13. Canaff L, Zhou X, Mosesova I, Cole DE, Hendy GN. Glial cells missing-2 (GCM2) transactivates the calcium-sensing receptor gene: effect of a dominant-negative GCM2 mutant associated with autosomal dominant hypoparathyroidism. *Hum Mutat.* 2009;**30**(1):85-92.

14. Mizobuchi M, Ritter CS, Krits I, Slatopolsky E, Sicard G, Brown AJ. Calcium-sensing receptor expression is regulated by glial cells missing-2 in human parathyroid cells. *J Bone Miner Res.* 2009;**24**(7):1173-1179.

15. Kumai Y, Kwong RW, Perry SF. A role for transcription factor glial cell missing 2 in Ca2+ homeostasis in zebrafish, *Danio rerio. Pflugers Arch.* 2015;**467**(4):753-765.

16. Fabbri S, Zonefrati R, Galli G, et al. In vitro control of genes critical for parathyroid embryogenesis by extracellular calcium. *J Endocr Soc.* 2020;**4**(7):bvaa058.

17. Su D, Ellis S, Napier A, Lee K, Manley NR. *Hoxa3* and *Pax1* regulate epithelial cell death and proliferation during thymus and parathyroid organogenesis. *Dev Biol.* 2001;**236**(2):316-329.

18. Peters H, Neubüser A, Kratochwil K, Balling R. *Pax9*-deficient mice lack pharyngeal pouch derivatives and teeth and exhibit craniofacial and limb abnormalities. *Genes Dev.* 1998;**12**(17):2735-2747.

19. Hackett JA, Surani MA. DNA methylation dynamics during the mammalian life cycle. *Philos Trans R Soc Lond B Biol Sci.* 2013;**368**(1609):20110328.

20. Christman JK. 5-Azacytidine and 5-aza-2′-deoxycytidine as inhibitors of DNA methylation: mechanistic studies and their implications for cancer therapy. *Oncogene.* 2002;**21**(35):5483-5495.

21. Fetahu IS, Höbaus J, Aggarwal A, et al. Calcium-sensing receptor silencing in colorectal cancer is associated with promoter hypermethylation and loss of acetylation on histone 3. *Int J Cancer.* 2014;**135**(9):2014-2023.

22. Singh P, Bhadada SK, Dahiya D, et al. Reduced calcium sensing receptor (CaSR) expression is epigenetically deregulated in parathyroid adenomas. *J Clin Endocrinol Metab.* 2020;**105**(9):3015-3024.

23. Yuan Y, Wang Q, Paulk J, et al. A small-molecule probe of the histone methyltransferase G9a induces cellular senescence in pancreatic adenocarcinoma. *ACS Chem Biol.* 2012;**7**(7):1152-1157.

24. Varshney S, Bhadada SK, Saikia UN, et al. Simultaneous expression analysis of vitamin D receptor, calcium-sensing receptor, cyclin D1, and PTH in symptomatic primary hyperparathyroidism in Asian Indians. *Eur J Endocrinol*. 2013;**169**(1):109-116.

25. Arya AK, Bhadada SK, Singh P, et al. Promoter hypermethylation inactivates CDKN2A, CDKN2B and RASSF1A genes in sporadic parathyroid adenomas. *Sci Rep*. 2017;**7**(1):3123.

26. Singh P, Vadi SK, Saikia UN, et al. Minimally invasive parathyroid carcinoma—a missing entity between parathyroid adenoma and carcinoma: scintigraphic and histological features. *Clin Endocrinol (Oxf)*. 2019;**91**(6):842-850.

27. RRID:AB_2891136.

28. Juhlin CC, Kiss NB, Villablanca A, et al. Frequent promoter hypermethylation of the APC and RASSF1A tumour suppressors in parathyroid tumours. *PLoS One*. 2010;**5**(3):e9472.

29. RRID:AB_306848.

30. RRID:AB_305237.

31. RRID:AB_823528.

32. Rahat B, Mahajan A, Bagga R, Hamid A, Kaur J. Epigenetic modifications at DMRs of placental genes are subjected to variations in normal gestation, pathological conditions and folate supplementation. *Sci Rep*. 2017;**7**:40774.

33. RRID:AB_2687657.

34. Fabbri S, Ciuffi S, Nardone V, et al. PTH-C1: a rat continuous cell line expressing the parathyroid phenotype. *Endocrine*. 2014;**47**(1):90-99.

35. RRID:AB_2877711.

36. Yamada T, Tatsumi N, Anraku A, et al. *Gcm2* regulates the maintenance of parathyroid cells in adult mice. *PLoS One*. 2019;**14**(1):e0210662.

37. Correa P, Akerström G, Westin G. Underexpression of *Gcm2*, a master regulatory gene of parathyroid gland development, in adenomas of primary hyperparathyroidism. *Clin Endocrinol (Oxf)*. 2002;**57**(4):501-505.

38. Kebebew E, Peng M, Wong MG, Ginzinger D, Duh QY, Clark OH. *GCMB* gene, a master regulator of parathyroid gland development, expression, and regulation in hyperparathyroidism. *Surgery*. 2004;**136**(6):1261-1266.

39. Guan B, Welch JM, Sapp JC, et al. *GCM2*-activating mutations in familial isolated hyperparathyroidism. *Am J Hum Genet*. 2016;**99**(5):1034-1044.

40. Guan B, Welch JM, Vemulapalli M, et al. Ethnicity of patients with germline *GCM2*-activating variants and primary hyperparathyroidism. *J Endocr Soc*. 2017;**1**(5):488-499.

41. Riccardi A, Aspir T, Shen L, et al. Analysis of activating *GCM2* sequence variants in sporadic parathyroid adenomas. *J Clin Endocrinol Metab*. 2019;**104**(6):1948-1952.

42. Ricketts CJ, Morris MR, Gentle D, et al. Methylation profiling and evaluation of demethylating therapy in renal cell carcinoma. *Clin Epigenetics*. 2013;**5**(1):16.

43. Chen Y, Bates DL, Dey R, et al. DNA binding by GATA transcription factor suggests mechanisms of DNA looping and long-range gene regulation. *Cell Rep*. 2012;**2**(5):1197-1206.

44. Chiofalo MG, Scognamiglio F, Losito S, Lastoria S, Marone U, Pezzullo L. Huge parathyroid carcinoma: clinical considerations and literature review. *World J Surg Oncol*. 2005;**3**:39.

45. Lalanne-Mistrih ML, Ognois-Ausse P, Goudet P, Cougard P. Giant parathyroid tumors: characterization of 26 glands weighing more than 3.5 grams [article in French]. *Ann Chir*. 2002;**127**(3):198-202.

46. Starlard-Davenport A, Tryndyak VP, James SR, et al. Mechanisms of epigenetic silencing of the *Rassf1a* gene during estrogen-induced breast carcinogenesis in ACI rats. *Carcinogenesis*. 2010;**31**(3):376-381.

47. Mossman D, Kim KT, Scott RJ. Demethylation by 5-aza-2′-deoxycytidine in colorectal cancer cells targets genomic DNA whilst promoter CpG island methylation persists. *BMC Cancer*. 2010;**10**:366.

48. Subramaniam D, Thombre R, Dhar A, Anant S. DNA methyltransferases: a novel target for prevention and therapy. *Front Oncol*. 2014;**4**:80.